PHYSICAL REVIEW C VOLUME 21, NUMBER 1 JANUARY 1980

Equilibrium statistical treatment of angular momenta associated with collective modes in fission and heavy-ion reactions

Luciano G. Moretto and Richard P. Schmitt
Lawrence Berkeley Laboratory, University of California, Berkeley, California 94720
(Received 14 May 1979)

The angular momentum effects in deep inelastic processes and fission have been studied in the limit of statistical equilibrium. The model consists of two touching liquid drop spheres. Angular momentum fractionation has been found to occur along the mass asymmetry coordinate. If neutron competition is included (i.e., in compound nucleus formation and fission), the fractionation occurs only to a slight degree, while extensive fractionation is predicted if no neutron competition occurs (i.e., in "fusion-fission" without compound nucleus formation). Thermal fluctuations in the angular momentum are predicted to occur due to degrees of freedom which can bear angular momentum such as wriggling, tilting, bending, and twisting. The coupling of relative motion to one of the wriggling modes, leading to fluctuations between orbital and intrinsic angular momentum, is considered first. Next the effect of the excitation of all the collective modes on the fragment spin is treated. General expressions for the first and second moments of the fragment spins are derived as a function of total angular momentum and the limiting behavior at large and small total angular momentum is examined. Furthermore, the effect of collective mode excitation on the fragment spin alignment is explored and is discussed in light of recent experiments. The relevance of the present study to the measured first and second moments of the γ-ray multiplicities as well as to sequential fission angular distributions is illustrated by applying the results of the theory to a well studied heavy-ion reaction.

[NUCLEAR REACTIONS Studied angular momentum fractionation along mass asymmetry mode. Investigated effect of collective rotational modes on fragment spins. Equilibrium statistical treatment.]

INTRODUCTION

Slowly, but unerringly, the study of heavy-ion reactions has brought problems involving angular momentum to the forefront of investigation. The untangling of the complex time evolution problems associated with heavy-ion reactions requires a good understanding of the relevant degrees of freedom and, to the extent to which angular momentum is involved, of the amount of angular momentum these degrees of freedom can carry. The importance of angular momentum in recent studies is illustrated by the work on gamma-ray multiplicities,[1-8] gamma-ray angular distributions,[9] and alpha[10] and sequential fission probabilities and angular distributions.[11-13] All of these topics have as a major theme the angular momentum and its partitioning among several, though not necessarily yet identified, degrees of freedom.

Transport equations have been advocated for the description of the time evolution of the intermediate complex formed in heavy-ion collisions and have even been applied with moderate success to the angular momentum transfer observed in these reactions.[14-16] However, the constant difficulty of the problem and the occasional occurrence in literature of *ad hoc* generalization of results to models with additional degrees of freedom not explicitly treated, has led us to the conclusion that a good deal could be learned by simplifying the problem in two ways: first, by making the model as simple as possible, striving to obtain transparent analytical results; second, by considering the long time limit of *statistical equilibrium*, to which all the transport equations must tend.

With the latter simplification we are, in a way, losing sight of the most exciting part of the game, namely the time dependence. However, we believe this to be a small and temporary sacrifice to make, considering the clarity of the results. Yet, even the statistical equilibrium limit is not deprived of interest. On the one hand, such a limit applies to all of the compound nucleus processes, fission in particular. On the other hand, many of the collective degrees of freedom which we consider are quite likely to be in most cases, either close to, or at the statistical equilibrium limit. There are, of course, most interesting and notable exceptions.

The plan of the paper is as follows: Section I deals with angular momentum fractionation along the mass asymmetry coordinate. As this degree of freedom is perhaps the slowest to equilibrate, this section is perhaps more relevant to fission than to deep-inelastic processes. Yet there exists, in heavy-ion reactions, components which

are apparently equilibrated along the mass asymmetry mode and yet are difficult to explain by compound nucleus decay.[17-20] It is possible that our formalism may enable one to learn about these components as well. Section II deals with the equilibrium partition of angular momentum between orbital and intrinsic rotation which involves the excitation of the collective modes known as wriggling.[21] In it both the average values and fluctuations are considered. The effect of the wriggling mode on the fragment spin alignment is discussed. Section III generalizes Sec. II by allowing the disintegration axis to tilt with respect to the plane normal to the total angular momentum. The average fragment angular momentum is obtained and the spin and angular fluctuations are estimated. In Sec. IV the thermal excitation of twisting and bending modes is studied for a system with zero total angular momentum. The average and rms angular momenta of the fragments are calculated. Section V generalizes Sec. IV by considering the twisting and bending modes in a system with a finite total angular momentum. The first and second moment of the fragment angular momentum as well as the fragment angular momentum depolarization are evaluated. In Sec. VI all of the above cases are considered for the reaction 600 MeV Kr + Au, and numerical estimates of angular momenta and their alignment are calculated.

It is hoped that this simple exercise in statistical mechanics will prove as useful to many heavy-ion practitioners, both theoretical and experimental, as it has been useful to us.

I. ANGULAR MOMENTUM FRACTIONATION ALONG THE MASS ASYMMETRY COORDINATE

Variations in the total exit-channel angular momentum along the mass asymmetry coordinate have been observed in nonequilibrium heavy-ion reactions.[5] In these processes the angular momentum fractionation appears to arise mainly from the decreasing rate of spread of the population along the mass asymmetry coordinate with increasing angular momentum due to the dependence of the interaction time upon angular momentum.

It is interesting to note that angular momentum fractionation is expected even when statistical equilibrium is attained along the ridge line, either directly as the end product of diffusion, or through population from the compound nucleus. The reason for this can easily be seen. For sufficiently heavy systems the potential as a function of mass asymmetry (ridge potential[22]) has a minimum at symmetry whose second derivative increases with increasing angular momentum. At equilibrium, the mass distributions for large angular momenta are more sharply peaked about symmetry than the mass distributions for small angular momenta. It follows that, after summation over all partial l waves, the average angular momentum decreases with increasing asymmetry. This is a straightforward prediction that can be easily verified. More quantitatively, let us consider the ridge line as a function of mass asymmetry and angular momenta. For two touching liquid-drop spheres of mass numbers A_1, A_2, the energy is

$$E=\tfrac{2}{5}E_R\frac{1}{x(1-x)[x^{1/3}+(1-x)^{1/3}]^2+\frac{2}{5}[x^{5/3}+(1-x)^{5/3}]}+E_C\left[\frac{5}{3}\frac{x(1-x)}{x^{1/3}+(1-x)^{1/3}}+x^{5/3}+(1-x)^{5/3}\right]$$
$$+E_S[x^{2/3}+(1-x)^{2/3}], \tag{1.1}$$

where E_R, E_C, E_S are the rotational, Coulomb, and surface energies of the equivalent sphere and $x=A_1/(A_1+A_2)$.

Expanding about $x=\frac{1}{2}$, we have

$$E=(0.453\,54+1.295\,84y^2)E_R+(0.892\,44+0.466\,64y^2)E_C+(1.259\,92-0.559\,96y^2)E_S=\alpha E_R+\beta E_C+\gamma E_S, \tag{1.2}$$

where $y=x-\frac{1}{2}$.

Incidentally, it may be of interest to note the value of the fissionability parameter, $X=E_C/2E_S$, at which the second derivative at symmetry is zero [Businaro-Gallone (BG) point]:

$$X_{\mathrm{BG}}=\tfrac{3}{5}-1.3885\frac{E_R}{E_S}. \tag{1.3}$$

Now let us assume that a compound nucleus has been formed and that neutron decay and fission are the only competing processes. In the constant temperature limit, dropping l-independent factors and assuming $\Gamma_T\cong\Gamma_N$, we get (see Appendix)

$$P(l,y) \propto \frac{\Gamma_F}{\Gamma_N}(l,y) \propto l \exp[-(RE_R + CE_C + SE_S)/T]dldy\,, \tag{1.4}$$

where $R=\alpha-1$, $C=\beta-1$, $S=\gamma-1$, and l is the angular momentum. Integrating over angular momentum we obtain for an entrance channel angular momentum distribution of the form $2l+1\cong 2l$

$$P(y) \propto \frac{T}{\Re E_R^{mx}}\left[\exp\left(-\frac{CE_C+SE_S}{T}\right)\right]\left[\exp\left(\Re\frac{E_R^{mx}}{T}-1\right)\right], \tag{1.5}$$

where E_R^{mx} is the maximum rotational energy of the equivalent sphere, and $\Re=-R$. The last equation can be written in terms of the fissionability parameter X and the rotational parameter $Y(X=E_C/2E_S,\ Y=E_R/E_S)$,

$$P(y) \propto \frac{1}{\Re}\exp\left(-\frac{2E_S(CX+\frac{1}{2}S)}{T}\right)\left[\exp\left(\frac{E_S}{T}\Re Y_{mx}\right)-1\right]. \tag{1.6}$$

The first moment of the angular momentum is

$$\bar{l}(y) = l_{mx}\frac{[1-(T/\Re E_R^{mx})^{1/2}F((\Re E_R^{mx}/T)^{1/2})]\exp(\Re E_R^{mx}/T)}{\exp(\Re E_R^{mx}/T)-1}, \tag{1.7}$$

where

$$F(x) = e^{-x^2}\int_0^x e^{y^2}dy$$

is the Dawson integral and l_{mx} is the maximum of the entrance channel angular-momentum distribution. The second moment of the angular momentum is

$$\bar{l}^2(y) = l_{mx}^2\frac{(1-T/\Re E_R^{mx})\exp(\Re E_R^{mx}/T)+T/\Re E_R^{mx}}{\exp(\Re E_R^{mx}/T)-1}. \tag{1.8}$$

These moments as well as the mass distributions as a function of the mass asymmetry y are shown in Figs. 1(a), 1(b).

From Fig. 1(a) one sees that the mass distributions for low values of l are considerably broader than those obtained for high l values. This is due to the fact that the minimum in the potential energy, which is shallow for the lower l values, becomes progressively deeper with increasing angular momentum, resulting in an increased concentration of the yield near symmetry. It is precisely this effect which leads to the fractionation of the angular momentum along the mass asymmetry coordinate [see Fig. 1(b)]. However, it is important to realize that the fissionability increases rapidly with l. This causes the distribution of angular momenta leading to fission to be narrower than the input triangular distribution and the overall average angular momentum leading to fission, $\bar{l}_D$, to be larger than that obtained by averaging over a triangular distribution. The resulting mass distribution, $P(y)$, is narrow and resembles the mass distributions obtained for the highest l-values.

With these points in mind, the interpretation of Fig. 1(b), which depicts $\bar{l}$ and $\bar{l}^2$ as a function of y, is fairly straightforward. For moderate values of y, both $\bar{l}/\bar{l}_D$ and $\bar{l}^2/\bar{l}_D{}^2$ are constant and close to unity. This is due to the fact that the high l waves dominate the yield for this range of asymmetries, so that averaging over l yields a value of $\bar{l},\bar{l}^2$, which is essentially $\bar{l}_D,\bar{l}_D{}^2$. However, the mass distributions for high l waves are relatively narrow, and as one moves out to extreme asymmetries their contribution to the total yield for a given asymmetry becomes less important, resulting in a slightly lower average l.

The constant temperature approximation is fairly poor. In particular, it is rather unwise to drop the dependence of T on angular momentum. Furthermore, the approximation $\Gamma_T\cong\Gamma_n$ fails when the fission width is large. At the expense of an analytic answer, a more accurate picture can be obtained by including the angular momentum dependence of T and by replacing Γ_n with $\Gamma_T=\Gamma_n+\Gamma_f$. The results are shown in Figs. 2(a),2(b). One sees that the mass distributions for the high l waves are narrower because of the lower temperature. On the other hand, the l-integrated mass distribution is somewhat broader because of the diminished weight given to the high l waves by the lower T and the division by Γ_T. These refinements cause $\bar{l},\bar{l}^2$ to drop off more as one moves to larger asymmetries [see Fig. 2(b)]. However, the qualitative interpretation is similar to that described above: $\bar{l},\bar{l}^2$ are nearly constant as a function of y for small y due to the dominance of the high l waves, and then drop off rather abruptly

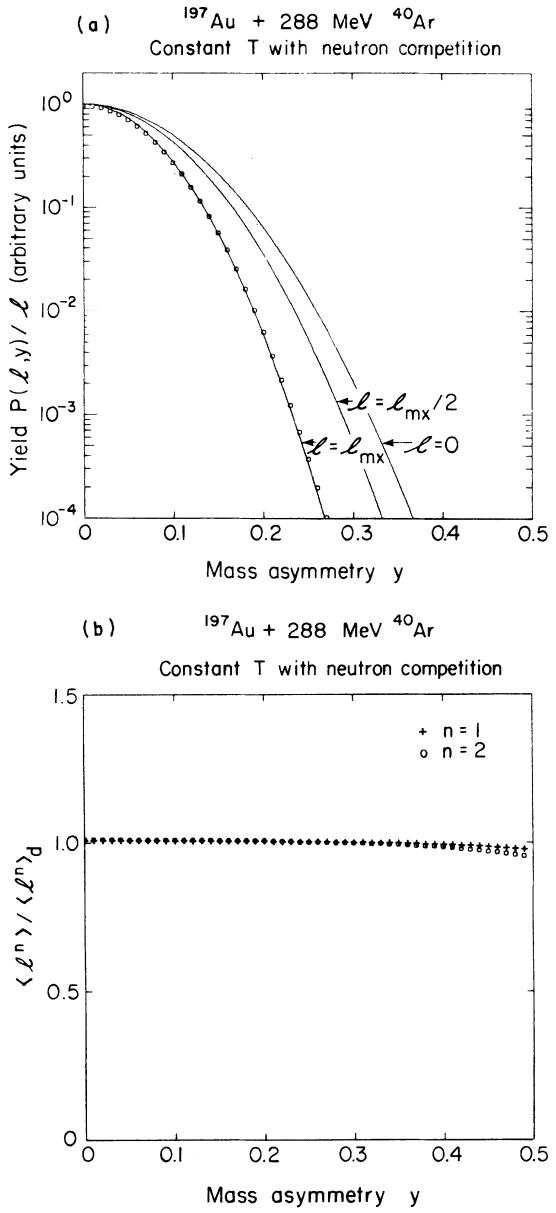

FIG. 1. (a) Calculated mass distributions for the indicated reaction obtained by integrating over all l waves leading to fission (squares) and for selected individual l waves (solid curves). All curves have been normalized to unity at symmetry. (b) Mean (crosses) and mean squared (squares) angular momentum as a function of mass asymmetry divided by the corresponding quantities obtained by integrating over the mass distribution.

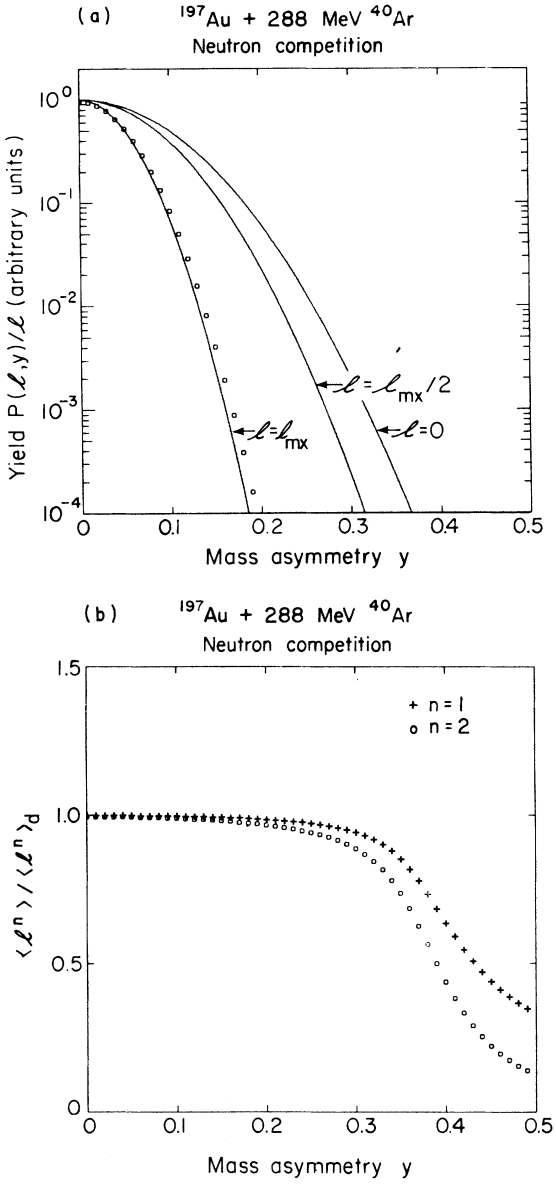

FIG. 2. (a) Same as Fig. 1(a) except that the angular momentum dependence of the temperature and total reaction width have been incorporated into the calculations (see text). (b) Same as Fig. 1(b) but including the same refinements as the calculation shown in Fig. 2(a).

because of the small contribution of the high l waves to the extreme asymmetries.

Another case which may be relevant in heavy-ion reactions arises when the system equilibrates along the ridge line and decays without passing through the compound nucleus stage. In other words, there is no competition from neutron emission or from other particle decay modes. In this case, Eqs. (1.4), (1.5), (1.7), (1.8) must be modified as follows:

$$P(l,y) = A(l.T)\, l \exp[-(RE_R + CE_C + SE_S)/T]\, dl\, dy\,, \tag{1.9}$$

where

$$A(l,T)=\left(\int \exp[-(RE_R+CE_C+SE_S)/T]dy\right)^{-1}.$$

Then

$$P(y)=\int P(l,y)dl \tag{1.10}$$

and

$$l(y)=\int lP(l,y)dl/P(y)\,, \tag{1.11}$$

$$l^2(y)=\int l^2P(l,y)dl/P(y)\,. \tag{1.12}$$

Notice that the difference between Eq. (1.4) and Eq. (1.9) resides only in the factor $A(l,T)$ which is absent in the former case and present in the latter. Calculations based upon this second set of equations are shown in Figs. 3(a),3(b). The mass distributions for the individual l waves shown in Fig. 3(a) are identical to those in Fig. 2(a) since the effect of neutron competition only changes the normalization (the mass distributions in the plots have all been normalized to unity to facilitate comparison). However, the distribution $P(y)$ is now considerably broader than its counterpart in Fig. 2(a) due to the change in the weighting of $P(l,y)$ in the integration over l.

The most significant effect of the assumption of equilibration along the ridge line can be seen in Fig. 3(b). In contrast to the preceding case (neutron competition), where $\overline{l}$ and $\overline{l^2}$ remained constant out to moderate asymmetries and then dropped off rapidly, $\overline{l}$ and $\overline{l^2}$ peak at symmetry and fall off more gradually with increasing y, giving rise to curves which are Gaussian in appearance. The dramatic differences in the l fractionation imply that it may be possible to distinguish between the two mechanisms, i.e., compound nucleus fission and noncompound nucleus decay, by measuring the angular momentum as a function of asymmetry. This result is particularly important in light of the fact that there are a number of examples[17-20] in heavy-ion reactions where fissionlike mass distributions occur which are difficult to explain in terms of compound nucleus decay, the reaction Xe + Fe being a recent example.[18] Moreover, recent γ multiplicity results[23] for the reaction Cu + Au bear a remarkable resemblance to the calculations in Fig. 3(b).

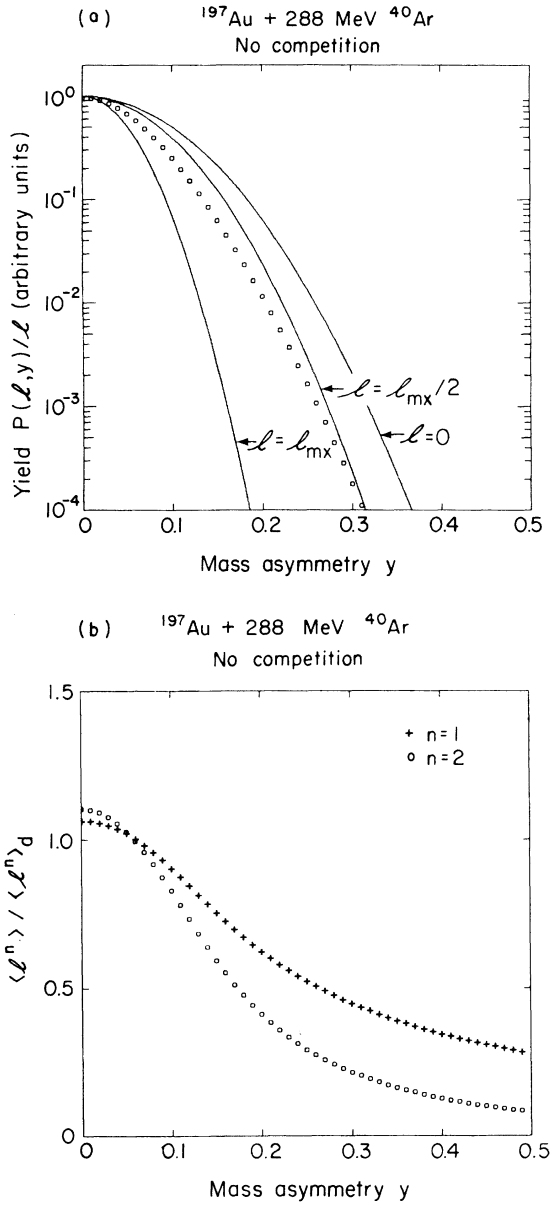

FIG. 3. (a) Same as Fig. 2(a) but in the absence of neutron competition. Note that only the total mass distribution (squares) is different from Fig. 2(a). (b) Same as Fig. 2(b) but without neutron competition.

II. STATISTICAL COUPLING BETWEEN ORBITAL AND INTRINSIC ANGULAR MOMENTA AND WRIGGLING MODES

In the spirit of simplicity let us assume that we can approximate the exit channel configuration by two touching, equal, rigid spheres with all the associated rotational degrees of freedom. As we shall see, this model leads to simple analytical predictions for the relevant statistical distributions. (In this model the normal modes do not have any restoring force and because of this it may be thought that some relevant physics may be missing. However, insofar as the angular momenta associated with these normal modes are concerned, the model does not suffer any limitation. This can be easily seen by observing that the angular momentum arises only from the

momentum component of the phase space which is indeed accounted for in the present model. The addition of restoring forces introduces a coordinate component of the phase space which would have to be integrated out.)

First, let us consider the equilibrium between intrinsic rotation of the fragments and their orbital rotation, assuming that the relevant angular momenta are all parallel to each other. If the total angular momentum is I and the fragment spin is s, the energy for an arbitrary partition between orbital and intrinsic angular momentum is

$$E(s)=\frac{(I-2s)^2}{2\mu r^2}+\frac{2s^2}{2\mathcal{I}}$$
$$=\left(\frac{2}{\mu r^2}+\frac{1}{\mathcal{I}}\right)s^2-\frac{2I}{\mu r^2}s+\frac{I^2}{2\mu r^2}. \tag{2.1}$$

The first term is the orbital and the second the intrinsic rotational energy, $\mathcal{I}$ being the moment of inertia of one of the two equal spheres.

The partition function is given by

$$Z\propto\int e^{-E(s)/T}ds$$
$$=\left(\frac{\pi\mu r^2\mathcal{I}T}{2\mathcal{I}+\mu r^2}\right)^{1/2}\exp\left(-\frac{I^2}{2T(2\mathcal{I}+\mu r^2)}\right). \tag{2.2}$$

The average spin for both fragments is given by

$$2\bar{s}=\frac{2\int se^{-E(s)/T}ds}{Z}$$
$$=\frac{2\mathcal{I}}{\mu r^2+2\mathcal{I}}I=\tfrac{2}{7}I=2I_R. \tag{2.3}$$

The second moment $\overline{s^2}$ is given by

$$4\overline{s^2}=\frac{2\mu r^2\mathcal{I}T}{\mu r^2+2\mathcal{I}}+\frac{4I^2\mathcal{I}^2}{(\mu r^2+2\mathcal{I})^2}. \tag{2.4}$$

From this we obtain the standard deviation

$$4\sigma_s^2=\frac{2\mathcal{I}\mu r^2T}{\mu r^2+2\mathcal{I}}=\frac{10}{7}\mathcal{I}T. \tag{2.5}$$

The result in (2.3) is temperature independent as one should have expected from the fact that (2.1) is quadratic in s. It could in fact be obtained by solving the equation

$$dE/ds=0. \tag{2.6}$$

This result corresponds to the mechanical limit of *rigid rotation* when the orbital and the intrinsic angular velocities are matched.

The result in (2.5) could have been obtained also by appreciating that the thermal fluctuations about the average in (2.3) are controlled by the second derivative of (2.1) at the minimum, or

$$\sigma_s^2=T/b, \tag{2.7}$$

where

$$b=\left[\frac{\partial^2E}{\partial s^2}\right]_{\bar{s}}.$$

It is important to appreciate the meaning of (2.5). The quantity $4\sigma^2$ represents the amount of angular momentum trade-off allowed by the temperature, between orbital and intrinsic rotation. It should correspond exactly to the long time limit of σ_z^2 of Ayik, Wolschin, and Nörenberg.[16] Just *because* of the meaning of this trade-off, it is unwarranted to assume *a priori* that similar values should be taken by σ_x^2 and σ_y^2, however defined (other orthogonal rotational modes), as implied in the same paper.

In some instances, such as γ-multiplicity measurements, one is interested in the average sum of the moduli of the fragment spins. This can be obtained from

$$2|\bar{s}|=\int 2|s|e^{-E(s)/T}ds/Z,$$

which yields

$$2|\bar{s}|=2\left\{\left(\frac{\mu r^2\mathcal{I}T}{\pi(\mu r^2+2\mathcal{I})}\right)^{1/2}\exp\left(-\frac{\mathcal{I}I^2}{\mu r^2T(\mu r^2+2\mathcal{I})}\right)\right.$$
$$\left.+I\frac{\mathcal{I}}{\mu r^2+2\mathcal{I}}\operatorname{erf}\left[I\left(\frac{\mathcal{I}}{\mu r^2T(\mu r^2+2\mathcal{I})}\right)^{1/2}\right]\right\}, \tag{2.8}$$

or, in dimensionless form,

$$\frac{2|\bar{s}|}{(\mathcal{I}^*T)^{1/2}}=2\left(\frac{1}{\sqrt{\pi}}\exp(-x^2)+x\operatorname{erf}(x)\right), \tag{2.9}$$

where $x=I_R/(\mathcal{I}^*T)^{1/2}$ and $\mathcal{I}^*=\mu r^2\mathcal{I}/(\mu r^2+2\mathcal{I})$. Also $I_R=I/7$ is the spin per fragment arising from rigid rotation. The above expression is plotted in Fig. 4. In the limit of large I, one recovers (2.3)

$$2|\bar{s}|=\frac{2\mathcal{I}I}{\mu r^2+2\mathcal{I}}=\tfrac{2}{7}I.$$

For small I,

$$\frac{2|\bar{s}|}{(\mathcal{I}^*T)^{1/2}}\simeq\frac{2}{\sqrt{\pi}}(1+x^2),$$

to order x^2, so for $I=0$ one obtains

$$2|\bar{s}|=2\left(\frac{\mathcal{I}T}{\pi}\right)^{1/2}\left(\frac{\mu r^2}{\mu r^2+2\mathcal{I}}\right)^{1/2}=2\left(\frac{5\mathcal{I}T}{7\pi}\right)^{1/2}. \tag{2.10}$$

The second moment, still given by Eq. (2.4) can be rewritten as $4\overline{s^2}=2\mathcal{I}^*T+4I_R^2$. In this case the fragment angular momentum at zero angular momentum arises from the excitation of a collective mode (wriggling[21]) in which the two fragments spin in the same direction while the system as a whole

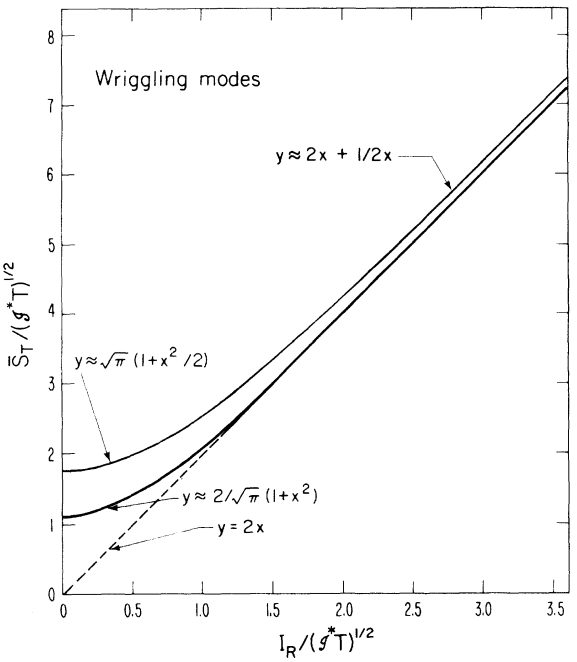

FIG. 4. Total spin of the fragments $\bar{S}_T = 2|\bar{S}|$ arising from wriggling as a function of the spin arising from rigid rotation alone plotted in dimensionless form. The upper solid curve shows the result for both of the wriggling modes while the lower solid curve corresponds to the excitation of a single wriggling mode (see text). The limiting behavior for both small and large x are indicated in both cases.

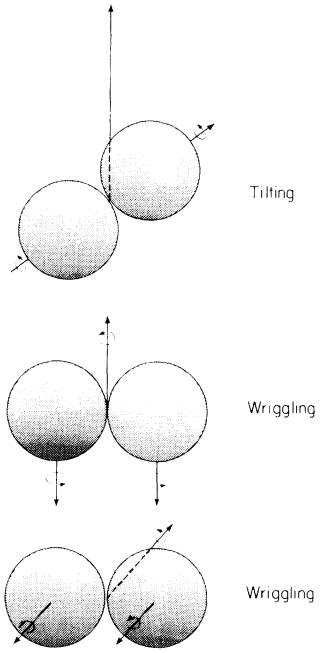

FIG. 5. Schematic illustrating the titling mode and the doubly degenerate wriggling modes for the two equal sphere model. The long arrows originating at the point of tangency for the two spheres is the orbital angular momentum while the shorter arrows represent the individual fragment spins.

rotates in the opposite direction in order to maintain $I=0$. Contrary to what has been assumed thus far, the wriggling mode is actually doubly degenerate, as illustrated in Fig. 5. Considering first the twofold degenerancy of the wriggling mode in the limit, $I=0$, one obtains

$$E(s)=\frac{s^2}{\mathcal{I}}+\frac{4s^2}{2\mu r^2}=\left(\frac{1}{\mathcal{I}}+\frac{2}{\mu r^2}\right)s^2=\frac{s^2}{\mathcal{I}^*}, \tag{2.11}$$

$$Z\propto \mathcal{I}^* T, \tag{2.12}$$

$$2|\bar{s}|=(\pi\mathcal{I}^* T)^{1/2}, \tag{2.13}$$

$$4\overline{s^2}=4\mathcal{I}^* T, \tag{2.14}$$

and

$$\sigma^2=(4-\pi)\mathcal{I}^* T. \tag{2.15}$$

Let us now couple this doubly degenerate mode to the spin arising from rigid rotation. If the aligned component of the angular momentum arising from rigid rotation is I_R and that due to wriggling is R, the total angular momentum for each fragment is

$$s^2=I_R^2+R^2+2I_R R\cos\theta. \tag{2.16}$$

The orbital angular momentum is

$$l_T^2=l^2+4R^2-4lR\cos\theta$$
$$=(I-2I_R)^2+4R^2-4(I-2I_R)R\cos\theta, \tag{2.17}$$

and the total energy is

$$E=\frac{35I_R^2+14R^2}{10\mathcal{I}}. \tag{2.18}$$

The partition function

$$Z\propto\int\int R\exp(-E/T)dRd\theta$$

is readily evaluated and yields

$$\ln Z=\ln\frac{\mathcal{I}T}{1.4}-\frac{3.5I_R^2}{\mathcal{I}T}+\text{const}. \tag{2.19}$$

The angular momentum of either fragment is

$$s=(I_R^2+R^2+2I_R R\cos\theta)^{1/2},$$

so the average sum of the moduli of the fragment spins is

$$2|\bar{s}|=\frac{2}{Z}\int\int(I_R^2+R^2+2I_R R\cos\theta)^{1/2}$$
$$\times R\exp(-E/T)dRd\theta. \tag{2.20}$$

The double integral in Eq. (2.20) cannot be evaluated in closed form. However, for large I_R and small I_R one can immediately obtain the integral

over θ:

$$2I_R+\frac{R^2}{2I_R} \quad \text{for } I_R \gg R\,,$$

$$2R+\frac{I_R^{\,2}}{2R} \quad \text{for } I_R \ll R\,.$$

The above are only limiting expressions, but they can be used as interpolation formulas from 0 to I_R and from I_R to ∞. Taken together the expressions above form a continuous function at $R=I_R$. The integral, moreover, is a continuous function along with its first derivative on the interval $(0,\infty)$ and yields a rather accurate approximation to $2|\bar{s}|$. It is given by

$$2|\bar{s}| = 2I_R+\frac{\mathcal{I}^*T}{2I_R}-\frac{1}{2}\left(I_R+\frac{\mathcal{I}^*T}{I_R}\right)\exp\left(-\frac{I_R^{\,2}}{\mathcal{I}^*T}\right) +\sqrt{\pi}\left((\mathcal{I}^*T)^{1/2}+\frac{I_R^{\,2}}{2(\mathcal{I}^*T)^{1/2}}\right)\operatorname{erfc}\left(\frac{I_R}{(\mathcal{I}^*T)^{1/2}}\right), \tag{2.21}$$

where again $\mathcal{I}^*=\mu r^2\mathcal{I}/(\mu r^2+2\mathcal{I})=\mathcal{I}/1.4$. In dimensionless form:

$$\frac{2|\bar{s}|}{(\mathcal{I}^*T)^{1/2}} = 2x+\frac{1}{2x}-\frac{1}{2}\left(x+\frac{1}{x}\right)\exp(-x^2) +\sqrt{\pi}\,(1+x^2/2)\operatorname{erfc}(x)\,. \tag{2.22}$$

This function, which is plotted in Fig. 4, has the following limiting values:

$$\frac{2|\bar{s}|}{(\mathcal{I}^*T)^{1/2}} = \sqrt{\pi}\left(1+\frac{x^2}{2}\right), \quad \text{small } I_R \tag{2.22a}$$

$$\frac{2|\bar{s}|}{(\mathcal{I}^*T)^{1/2}} = 2x+\frac{1}{2x}, \quad \text{large } I_R\,. \tag{2.22b}$$

Also in the limit of large I_R, one obtains

$$4\sigma^2 = 4I_R^{\,2}+4\overline{R^2}-4I_R^{\,2}-2\overline{R^2}=2\overline{R^2}=2\mathcal{I}^*T\,, \tag{2.23}$$

where $\overline{R^2}=\mathcal{I}^*T$.

It is interesting to note that the wriggling mode generates a random angular momentum *in a plane perpendicular to the line of centers of the fragments*. The vector sum of this random angular momentum and that arising from rigid rotation thus leads to a fluctuation in the orientation of the total spin, again *in the plane perpendicular to the separation axis*. The corresponding rms angle is easily obtained from

$$\tan\theta \simeq \left(\frac{\overline{R^2}}{I_R^{\,2}}\right)^{1/2}=\left(\frac{\mathcal{I}^*T}{I_R^{\,2}}\right)^{1/2}=\left(\frac{5\mathcal{I}T}{7I_R^{\,2}}\right)^{1/2}. \tag{2.24}$$

Now let us consider the effect of this spin depolarization on the in-plane and out-of-plane angular distributions of fission fragments produced via the sequential decay of heavy products produced by deep-inelastic collisions. (The fission process itself can lead to an out-of-plane width,[23] although one need not consider that in this discussion.) If the recoiling nucleus fissions perpendicular to the separation axis in a plane perpendicular to its spin, then wriggling will contribute to the out-of-plane anisotropy via Eq. (2.24). On the other hand, if the fission occurs along the separation axis, the wriggling process will have no effect on the out-of-plane width; however, an in-plane anisotropy will be generated due to the intersection of all possible fission decay planes along the original separation axis.

Interestingly enough, a depolarization of the type discussed above has been employed in calculations aimed at reproducing sequential fission data for Kr + Bi,[11] where an in-plane anisotropy has been observed experimentally. However, it is not possible to attribute the in-plane anisotropy to wriggling alone since other measurements[13] have not shown any appreciable variation in the out-of-plane width with the in-plane angle.

At any rate, the fragment spin depolarization arises from other sources as well, as will be discussed in the next chapters.

III. THERMAL FLUCTUATION OF THE ANGULAR MOMENTUM PROJECTION ON THE DISINTEGRATION AXIS: TILTING

Above, we have assumed that the two touching fragments are aligned with their common axis perpendicular to the total angular momentum. Because of the thermal fluctuations, this condition can be relaxed (see Fig. 5). Assuming now that the two fragments are rigidly attached one to the other, the energy is given by

$$E=\frac{I^2-K^2}{2\mathcal{I}_\perp}+\frac{K^2}{2\mathcal{I}_\parallel}=\frac{I^2}{2\mathcal{I}_\perp}+\frac{K^2}{2\mathcal{I}_{\rm eff}} \tag{3.1}$$

where $\mathcal{I}_\perp=2\mathcal{I}+\mu r^2$; $\mathcal{I}_\parallel=2\mathcal{I}$; and $\mathcal{I}_{\rm eff}^{-1}=\mathcal{I}_\parallel^{-1}-\mathcal{I}_\perp^{-1}$; K is the projection of the angular momentum I along the line of centers. The partition function is

$$Z=\sqrt{\pi}\exp(-I^2/2\mathcal{I}_\perp T)(2\mathcal{I}_{\rm eff}T)^{1/2}\operatorname{erf}[I/(2\mathcal{I}_{\rm eff}T)^{1/2}] \tag{3.2}$$

from which

$$\overline{K^2}=\mathcal{I}_{\rm eff}T-\frac{I(2\mathcal{I}_{\rm eff}T)^{1/2}}{\sqrt{\pi}}\,\frac{\exp(-I^2/2\mathcal{I}_{\rm eff}T)}{\operatorname{erf}[I/(2\mathcal{I}_{\rm eff}T)^{1/2}]}\,. \tag{3.3}$$

For small I we have

$$\overline{K^2}=\tfrac{1}{3}I^2\,, \tag{3.4a}$$

while for large I we have

$$\overline{K^2}=\mathcal{I}_{\rm eff}T=\tfrac{14}{5}\mathcal{I}T\,. \tag{3.4b}$$

The total fragment spin is given by

$$2s=[K^2+\tfrac{4}{49}(I^2-K^2)]^{1/2}\,, \tag{3.5}$$

and the averaged square quantity is

$$4\overline{s^2}=\overline{K^2}+\tfrac{4}{49}I^2-\tfrac{4}{49}\overline{K^2}=\tfrac{45}{49}\overline{K^2}+\tfrac{4}{49}I^2, \tag{3.6a}$$

and for large I,

$$4\overline{s^2}=\tfrac{18}{7}\mathcal{I}T+\tfrac{4}{49}I^2. \tag{3.6b}$$

The average, on the other hand, is

$$\begin{aligned}2\overline{s}&=\frac{\int\frac{2}{7}\mathcal{I}(1+\frac{45}{4}K^2/I^2)^{1/2}e^{-E/T}dK}{Z}\\&\approx\tfrac{2}{7}I+\frac{\int\frac{45}{28}(K^2/I)e^{-E/T}dK}{Z}\\&=\frac{2}{7}I+\tfrac{45}{28}\frac{\overline{K^2}}{I}=\frac{2}{7}I\left(1+\frac{45}{8}\frac{\overline{K^2}}{I^2}\right)=2I_R+\frac{9}{14}\frac{\mathcal{I}T}{I_R},\end{aligned} \tag{3.7}$$

where we have dropped terms of order higher than $\overline{K^2}/I^2$. From the above equations one learns that the total angular momentum of the fragments is only slightly affected by the thermal fluctuations of the separation axis and that the correction to the ordinary rigid rotation limit, at constant temperature, decreases as I^{-1}. Furthermore, the fluctuation $\sigma^2\cong 0$ up to order K^2/I^2 and can be neglected in most cases.

Because of the excitation of this mode the reaction plane is not perpendicular to the total angular momentum of the system I, but is "tilted" by an angle θ_t given by

$$\sin\theta_t=\left(\frac{\overline{K^2}}{I^2}\right)^{1/2}. \tag{3.8}$$

The angle more relevant to sequential fission angular distributions is the angle between the total spin of one fragment and the normal to the line of centers (in the same plane as I), which is given by

$$\sin\theta=\left(\frac{\overline{K^2}}{4\overline{s^2}}\right)^{1/2}. \tag{3.9}$$

Since I may be considerably larger than s, this angle can be considerably larger than θ_t. One should note that the combined effect of wriggling and tilting will produce spin components along all the coordinate axes. If the separation axis is the z axis, tilting will lead to an rms z component of $(\overline{K^2}/4)^{1/2}=0.84\sqrt{\mathcal{I}T}$ for each fragment. On the other hand, the rms x and y components due to wriggling will be $(\overline{R^2}/2)^{1/2}=0.60\sqrt{\mathcal{I}T}$; hence, tilting and wriggling together generate an angular momentum which is almost random.

IV. TWISTING AND BENDING MODES EXCITED IN A ZERO-ANGULAR-MOMENTUM SYSTEM

These three degrees of freedom are illustrated in Fig. 6. They are degenerate in our two-equal-sphere model.[12] A splitting of the degeneracy could easily occur in the case of fragment deformation. We shall not consider this rather important possibility at the moment, although it is completely trivial, because of the arbitrariness in the choice of deformation.

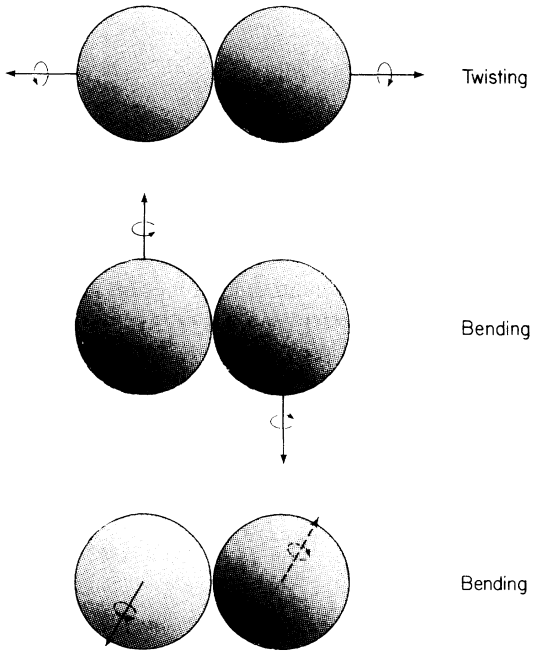

FIG. 6. Schematic illustrating the twisting and bending modes for the two-equal-sphere model. Note the pairwise cancellation of the fragment spins.

The partition function can be written as

$$Z\propto\int R^2\exp(-R^2/\mathcal{I}T)dR \tag{4.1}$$

and

$$\ln Z=A-\tfrac{3}{2}\ln\frac{1}{\mathcal{I}T} \tag{4.2}$$

from which

$$\overline{R}=\frac{2}{\sqrt{\pi}}(\mathcal{I}T)^{1/2}, \tag{4.3}$$

$$\overline{R^2}=-\frac{\partial\ln Z}{\partial[1/\mathcal{I}T]}=\tfrac{3}{2}\mathcal{I}T \tag{4.4}$$

and

$$\sigma_R{}^2=\left(\frac{3}{2}-\frac{4}{\pi}\right)\mathcal{I}T\cong 0.227\mathcal{I}T. \tag{4.5}$$

Notice that R is the angular momentum of *each* fragment and that, for each mode, the angular momenta of the two fragments cancel out pairwise. Furthermore, for each fragment the resulting angular momentum is randomly oriented. It is worth stressing again that this angular momentum can exist even when the total angular mo-

mentum is zero because of the pairwise cancellation mentioned above.

V. COUPLING OF TWISTING AND BENDING MODES TO RIGID ROTATION

We want to generalize the previous calculation to the case of nonzero total angular momentum. Let us assume that *each* fragment has an aligned angular momentum component I_R arising from rigid rotation and a random component R due to the bending and twisting modes. The overall rotational energy arising from the fragment spins is

$$E=\frac{1}{2\mathcal{I}}\left[(I_R^2+R^2+2RI_R\cos\theta)+(I_R^2+R^2-2RI_R\cos\theta)\right]=\frac{1}{\mathcal{I}}(I_R^2+R^2)\,. \tag{5.1}$$

The average total angular momentum of the fragments is

$$2|\bar{s}|=\frac{2\pi\int\int\left[(I_R^2+R^2+2I_RR\cos\theta)^{1/2}+(I_R^2+R^2-2I_RR\cos\theta)^{1/2}\right]R^2\exp(-R^2/\mathcal{I}T)dR\sin\theta\,d\theta}{2\pi\int\int R^2\exp(-R^2/\mathcal{I}T)dR\sin\theta\,d\theta}\,. \tag{5.2}$$

The integral over θ yields

$$2I_R+\frac{2}{3}\frac{R^2}{I_R}\quad\text{for } I_R>R\,,$$

$$2R+\frac{2}{3}\frac{I_R^2}{R}\quad\text{for } I_R<R\,.$$

Thus caution is necessary in calculating the thermal average. The result is

$$2|\bar{s}|=\left(2I_R+\frac{\mathcal{I}T}{I_R}\right)\mathrm{erf}(I_R/\sqrt{\mathcal{I}T})+\frac{2}{\sqrt{\pi}}\sqrt{\mathcal{I}T}\exp(-I_R^2/\mathcal{I}T)\,. \tag{5.3}$$

This expression can be written in dimensionless form as

$$\frac{2|\bar{s}|}{\sqrt{\mathcal{I}T}}=\left(2x+\frac{1}{x}\right)\mathrm{erf}(x)+\frac{2}{\sqrt{\pi}}\exp(-x^2)\,, \tag{5.4}$$

where $x=I_R/\sqrt{\mathcal{I}T}$. This function is plotted in Fig. 7. For small x one obtains

$$\frac{2|\bar{s}|}{\sqrt{\mathcal{I}T}}\cong\frac{4}{\sqrt{\pi}}\left(1+\frac{x^2}{3}\right). \tag{5.5}$$

In the limit of $I_R=0$, one obtains

$$2|\bar{s}|=\frac{4}{\sqrt{\pi}}\sqrt{\mathcal{I}T}=2\bar{R} \tag{5.6}$$

in agreement with the results of the last section. For large x,

$$\frac{2|\bar{s}|}{\sqrt{\mathcal{I}T}}\cong 2x+\frac{1}{x} \tag{5.7}$$

or

$$2|\bar{s}|=2I_R+\frac{\mathcal{I}T}{I_R}=2I_R+\frac{2}{3}\frac{\overline{R^2}}{I_R}=\frac{2}{7}I\left(1+\frac{49}{2}\frac{\mathcal{I}T}{I^2}\right). \tag{5.8}$$

Similarly the average square angular momentum is

$$4\overline{s^2}=2I_R^2+2\overline{R^2}+2\int\left[\frac{1}{2}(I_R^4+R^4-2I_R^2R^2)^{1/2}+\frac{(I_R^2+R^2)^2}{4RI_R}\sin^{-1}\left(\frac{2I_RR}{I_R^2+R^2}\right)\right]R^2\exp\left(-\frac{R^2}{\mathcal{I}T}\right)dR\,, \tag{5.9}$$

which, to order $\overline{R^2}/I_R^2$, yields

$$4\overline{s^2}=4(I_R^2+\overline{R^2})\,, \tag{5.10}$$

$$4\sigma^2=\tfrac{4}{3}\overline{R^2}=2\mathcal{I}T\,. \tag{5.11}$$

In this case as well as in (3.7) and (2.22b) we see that the correction to the rigid rotation limit decreases as I^{-1} in Eq. (5.8), but with a slightly larger coefficient. However, there is some appreciable contribution to the width. Of greatest importance is the fact that a sizeable "tilt" of the angular momentum of each fragment about the direction of the total angular momentum is introduced

$$\tan\theta\cong\left(\frac{\overline{R^2}}{I_R^2}\right)^{1/2}=\left(\frac{3\mathcal{I}T}{2I_R^2}\right)^{1/2}. \tag{5.12}$$

This depolarization is of great importance for the proper interpretation of the out-of-plane angular distribution of gamma rays emitted by the fragments and of the out-of-plane angular distribution of sequential fission fragments.[12] Note that the effect on the depolarization in Eq. (5.12) is larger than that due to tilting in Eq. (2.24).

VI. A SIMPLE APPLICATION TO A TYPICAL HEAVY-ION REACTION

It should be stressed again that the above formalism applies strictly to a system which has reached statistical equilibrium. In general this is not the case in heavy-ion reactions, especially insofar as the mass asymmetry degree of freedom

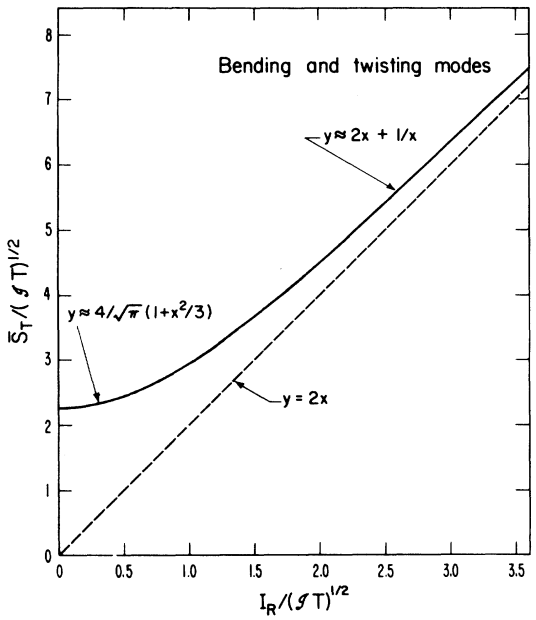

FIG. 7. Total fragment spin $\bar{S}_T = 2|\bar{S}|$ as a function of the spin arising from rigid rotation for the twisting and bending modes. Dimensionless forms are utilized. The limiting behavior for large and small x are indicated.

is concerned. However, for other degrees of freedom statistical equilibrium may be reached or closely approached. At any rate, it is interesting to compare the predictions of an equilibrium model with experiment.

The reaction which we want to consider is 600 MeV ^{86}Kr + ^{197}Au. Some of the vital statistics of this reaction are summarized in Table I. If we allow the system to evolve to the configuration of two touching spheres $[r = 1.22(A_2^{1/3} + A_2^{1/3}) + 2]$ we have (either for $l_{\rm rms}$ or $\bar{l}$) an excitation energy of 113 MeV, so $T = 1.78$ MeV and $\mathcal{I}T = 131\hbar^2$ or $\sqrt{\mathcal{I}T} \cong 12\hbar$.

Now let us first consider the effect of the doubly degenerate wriggling mode. For the average angular momentum the total spin is given by Eq. (2.22b),

TABLE I. 600 MeV ^{86}Kr + ^{197}Au.

$E_{\rm lab}$	= 600 MeV
$E_{\rm c.m.}$	= 418 MeV
$B_{\rm Coul}$	= 283 MeV
$E/B_{\rm Coul}$	= 1.48
$l_{\rm max}$	= 285$\hbar$
$l_{\rm rms}$	= 202
$\bar{l}$	= 190

$$2|\bar{s}| = \frac{2}{7}190 + \frac{7}{2}\frac{93.75}{190}$$
$$= 54.29 + 1.73 = 56.02\hbar$$

and from Eq. (2.23),

$$4\sigma^2 = 2(93.75) = 187.50\hbar^2 .$$

The fluctuation of the separation axis with respect to the total angular momentum yields the following from Eqs. (3.4b) and (3.7):

$$\overline{K^2} = \tfrac{14}{5}\mathcal{I}T = 367.50\hbar^2 ,$$
$$2\bar{s} = \frac{2}{7}190 + \frac{9}{2}\frac{131.25}{190}$$
$$= 54.29 + 3.11 = 57.40\hbar .$$

The out-of-plane tilting of the separation axis from Eq. (3.8) is

$$\theta = \sin^{-1}\left(\frac{\sqrt{367.50}}{190}\right) = 5.79^\circ .$$

Since wriggling and tilting together produce an angular momentum which is nearly random we can estimate their combined effect on the depolarization of the fragment spin from Eq. (3.9)

$$\theta = \sin^{-1}\left(\frac{\frac{1}{2}\sqrt{367.50}}{28.70}\right) = 19.51^\circ$$

which is indeed substantial. The twisting and bending modes lead to

$$\overline{R^2} = \tfrac{3}{2}\mathcal{I}T = 196.88\hbar^2 ,$$
$$2\bar{s} = \tfrac{2}{7}190 + 7\,\frac{131.25}{190}$$
$$= 54.29 + 4.84 = 59.13\hbar ,$$
$$4\sigma^2 = 2(131.25) = 262.50\hbar^2 .$$

This produces an angular momentum depolarization of

$$\theta = \tan^{-1}\left(\frac{\sqrt{196.88}}{27.14}\right) = 27.34^\circ .$$

The combination of wriggling, tilting, bending, and twisting gives rise to an overall nearly isotropic angular momentum depolarization of $\theta \cong 34^\circ$. Recent measurements of out-of-plane sequential fission angular distributions for Au + Kr[12] give a width of ~25°. This is not necessarily at variance with the value of 34° just calculated, because sequential fission will favor the larger angular momenta, resulting in a smaller depolarization.

A depolarization of ~34° is also quite helpful in explaining the small out-of-plane anisotropies in the gamma rays associated with deep inelastic processes. A 30% to 70% split in the $E1$,$E2$ con-

tributions added to the above depolarization are sufficient to explain the 10% to 30% anisotropies observed.

If one assumes a triangular distribution for the angular momentum distribution (i.e., no l fractionation), there is an additional contribution to the sigma squared of both fragments of

$$4\sigma^2=\frac{4}{49}\left(\frac{l_{\max}{}^2}{2}-\frac{4}{9}l_{\max}{}^2\right)=368.37\hbar^2 .$$

Summing all the fluctuations we obtain

$$4\sigma^2=818.37\hbar^2 \text{ or } 2\sigma=28.61\hbar .$$

In conclusion, without allowing for angular momentum fractionation, we obtain for the overall fragment spin

$$2|\bar{s}|\cong 64\pm 29\hbar .$$

Another interesting case is spin generated by the wriggling, bending, and twisting modes for zero total angular momentum. For wriggling we obtain

$$2|\bar{s}|=(\pi\vartheta^* T)^{1/2}=17.16\hbar .$$

Bending and twisting contribute

$$2\bar{s}=\frac{4}{\sqrt{\pi}}\sqrt{\vartheta T}=25.85\hbar .$$

Combining both angular momenta one obtains

$$(\overline{s^2})^{1/2}=15.5\hbar$$

for each fragment.

VII. CONCLUSION

In conclusion, using a simple model we have investigated the angular momenta associated with a number of collective degrees of freedom. For the mass-asymmetry mode we have found that there can be appreciable l fractionation along the mass-asymmetry coordinate, even in the equilibrium limit. Furthermore, the distinctly different patterns observed for the case of compound-nucleus decay and for non-compound-nucleus decay (i.e., equilibration along the ridge line) imply that it may be possible to experimentally distinguish between these two mechanisms, perhaps via γ-ray multiplicity measurements. Six other collective modes have been considered: two wriggling, one tilting, two bending, and one twisting. Excitation of these modes causes a modest increase in the average fragment spins over the rigid rotational value, but leads to a sizeable spread in the fragment's angular momenta about the average value. In addition, these modes also result in a depolarization of the fragment spins and induce significant spin in the fragments for zero total angular momentum.

Comparisons with experimental results are, of course, welcome and left to the readers. To many the agreement may appear remarkable. However, we caution against excessive confidence in view of the crudeness of the model. Yet we hope that the wise use of this exercise (*cum grano salis*) may help in understanding the much more intricate aspects of everyday life in fission and heavy-ion reactions.

APPENDIX

The general expression for the ratio of the fission width Γ_F to the neutron width Γ_N is[25]

$$\frac{\Gamma_F}{\Gamma_N}=\frac{\pi\hbar^2}{4\sigma_{\text{inv}}m_N}\frac{\int\rho_F(E-B_F-E_F^R-\epsilon)d\epsilon}{\int\epsilon\rho_N(E-B_N-E_N^R-\epsilon)d\epsilon}, \tag{A1}$$

where σ_{inv} is the neutron cross section for the inverse reaction; m_N is the neutron mass; ϵ is the neutron kinetic energy or the kinetic energy along the fission mode at the saddle; B_F and B_N are the fission barrier height and the neutron binding energies, respectively; E_F^R and E_N^R are the rotational energies at the fission saddle point and for the residual nucleus after neutron emission, respectively; and Γ_F and Γ_N are the level densities at the saddle point and of the residual nucleus after neutron emission, respectively.

By expanding $\ln\rho$ in power series to first order in ϵ the integrals can be performed to give

$$\frac{\Gamma_F}{\Gamma_N}=\frac{\pi\hbar^2}{4\sigma_{\text{inv}}m_N}\frac{T_F}{T_N{}^2}\frac{\rho_F(E-B_F-E_F^R)}{\rho_N(E-B_N-E_N^R)}, \tag{A2}$$

where

$$\frac{1}{T_F}=\frac{\partial\ln\rho_F}{\partial\epsilon};\quad\frac{1}{T_N}=\frac{\partial\ln\rho_N}{\partial\epsilon},$$

both derivatives being evaluated at the upper limit of the respective integrals. This expression can be simplified by further expanding $\ln\rho$ in power series and by setting $T_F\cong T_N=T$

$$\frac{\Gamma_F}{\Gamma_N}\cong\frac{\pi\hbar^2}{4\sigma_{\text{inv}}M_N}\frac{1}{T}\frac{\rho_F(E)}{\rho_N(E)}\exp\left(-\frac{B_F+E_F^R-B_N-E_N^R}{T}\right). \tag{A3}$$

The dependence of Γ_F on the mass asymmetry y can be easily introduced in the above expression by a minor redefinition of ρ_F

$$\frac{\Gamma_F(y)}{\Gamma_N}\cong\frac{\hbar^2}{4\sigma_{\text{inv}}M_N}\frac{1}{T}\frac{\rho_F'(E)}{\rho_N(E)}\times\exp\left(-\frac{B_F(y)+E_F^R(y)-B_N-E_N^R}{T}\right). \tag{A4}$$

The ratio $\rho_F'(E)/\rho_N(E)$ is approximately constant and close to unity. By retaining explicitly only the angular-momentum-dependent factors, one

obtains

$$\frac{\Gamma_F(y)}{\Gamma_N} \propto \exp\left(-\frac{B_F(y)+E_F^R-E_N^R}{T}\right) \qquad \text{(A5)}$$

which is immediately identifiable with the expression (1.4) apart from the statistical weight l to be included when an impact parameter integration is considered. It should be appreciated that the level-density expansion introduced to obtain (A2) and (A3) is not a mere technicality. One can see that all the statistical mechanics of the system, initially residing in the level densities ("microcanonical" description) now resides in the coefficients of the first order expansion of their logarithms in $1/T$. This is called the "canonical" expansion and it allows one to describe with a single parameter T the statistical equilibrium between a limited number of explicitly treated degrees of freedom (fission mode; neutron translational degrees of freedom) and the large number of the remaining internal degrees of freedom. In the wide range of excitation energies in which such an expansion is a good approximation, the remaining degrees of freedom can be considered a "thermostat" or a "heat bath" whose temperature is T. The canonical expansion is used widely throughout the paper and its advantages in reducing a variety of problems to a form amenable to analytical treatment are hopefully apparent.

Finally it should be stressed that one should never say that a nucleus has a given temperature T. In fact, for an isolated nucleus ρ and not T is the relevant statistical quantity. Rather one should say that the statistical equilibrium between a given set of collective models and the remaining intrinsic modes is characterized by a temperature T.

[1]R. Albrecht, W. Dünnweber, G. Graw, H. Ho, S. A. Steadman, and J. P. Wurm, Phys. Rev. Lett. 34, 1500 (1975).

[2]M. Ishihara, J. Numao, T. Fukada, K. Tanaka, and T. Inamura, in *Proceedings of the Symposium on Macroscopic Features of Heavy-Ion Collisions, Argonne, Illinois, 1976*, edited by D. G. Kovar, ANL Report No. ANL-PHY-76-2, p. 617.

[3]P. Glässel, R. S. Simon, R. M. Diamond, R. C. Jared, I. Y. Lee, L. G. Moretto, J. O. Newton, R. Schmitt, and F. S. Stephens, Phys. Rev. Lett. 38, 331 (1977).

[4]M. Berlanger, M. A. Deleplanque, C. Gerschel, F. Hanappe, M. LeBlanc, J. F. Mayault, C. Ngô, D. Paya, N. Perrin, J. Péter, B. Tamain, and L. Valentin, J. Phys. Lett. L37, 323 (1976).

[5]M. M. Aleonard, G. J. Wozniak, P. Glässel, M. M. Deleplanque, R. M. Diamond, L. G. Moretto, R. P. Schmitt, and F. S. Stephens, Phys. Rev. Lett. 40, 622 (1978).

[6]J. B. Natowitz, M. N. Namboodiri, P. Kasiraj, R. Eggers, L. Alder, P. Gouthier, C. Cerruti, and T. Alleman, Phys. Rev. Lett. 40, 751 (1978).

[7]P. R. Christensen, F. Folkmann, O. Hansen, O. Nathan, N. Trautner, F. Videbaek, S. Y. van der Werf, H. C. Britt, R. P. Chestnut, H. Freiesblehen, and F. Pühlhofer, Phys. Rev. Lett. 40, 1245 (1978).

[8]A. Olmi, H. Sann, D. Pelte, Y. Eval, A. Gobbi, W. Kohl, U. Lynen, G. Rudolf, H. Stelzer, and R. Bock, Phys. Rev. Lett. 41, 688 (1978).

[9]R. A. Dayras, R. G. Stokstad, C. B. Fulmer, D. C. Hensley, M. L. Halbert, R. L. Robinson, A. H. Snell, D. G. Sarantites, L. Westerberg, and J. H. Barber, Phys. Rev. Lett. 42, 697 (1979).

[10]H. Ho, R. Albrecht, W. Dünnweber, G. Graw, S. G. Steadman, J. P. Wurm, D. Disdier, V. Rauch, and F. Scheibling, Z. Phys. A283, 234 (1977).

[11]P. Dyer, R. J. Puigh, R. Vandenbosch, T. D. Thomas, and M. S. Zisman, Phys. Rev. Lett. 39, 392 (1977).

[12]G. J. Wozniak, R. P. Schmitt, P. Glassel, J. C. Jared, G. Bizard, and L. G. Moretto, Phys. Rev. Lett. 40, 1436 (1978).

[13]H. J. Specht, in Proceedings of the International Conference on Nuclear Interactions, Australian Academy of Science, Canberra City, Australia, 1978 (unpublished).

[14]R. Regimbart, A. N. Behkami, G. J. Wozniak, R. P. Schmitt, J. S. Sventek, and L. G. Moretto, Phys. Rev. Lett. 41, 1355 (1978).

[15]G.Wolschin and W. Nörenberg, Phys. Rev. Lett. 41, 691 (1978).

[16]S. Ayik, G. Wolschin and W. Nörenberg, Z. Phys. A286, 271 (1978).

[17]L. G. Moretto, J. Galin, R. Babinet, Z. Fraenkel, R. Schmitt, R. Jared, and S. G. Thompson, Nucl. Phys. A259, 172 (1976).

[18]B. Heusch, C. Volant, H. Freiesleben, R. P. Chestnut, K. D. Hildenbrand, F. Pühlhofer, W. F. W. Schneider, B. Kohlmeyer, and W. Pfeffer, Z. Phys. A288, 391 (1978).

[19]J. Galin, B. Gatty, D. Guerrean, M. Lefort, X. Tarrago, S. Agarwal, R. Babinet, B. Cauvin, J. Girard, and H. Nifenecker, Z. Phys. A283, 173 (1977).

[20]M. Beckerman and M. Blann, Phys. Rev. Lett. 38, 272 (1977).

[21]J. R. Nix and W. J. Swiatecki, Nucl. Phys. 71, 1 (1965).

[22]L. G. Moretto, Nucl. Phys. A247, 211 (1975).

[23]C. Gerschel, M. A. Delephanque, M. Isihara, C. Ngô, N. Perrin, J. Péter, B. Tamain, L. Valentin, D. Paya, Y. Sugiyama, M. Berlanger, and F. Hanappe, Nucl. Phys. A317, 473 (1979).

[24]R. Vandenbosch and J. R. Huizenga, *Nuclear Fission* (Academic, New York, 1973), p. 180.

[25]For an extensive description of the expressions for the neutron and fission widths, see L. G. Moretto, *Physics and Chemistry of Fission, 1973* (IAEA, Vienna, 1974), Vol. 1, p. 329.

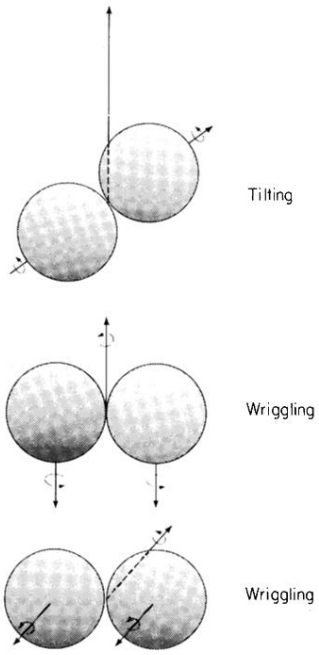

FIG. 5. Schematic illustrating the titling mode and the doubly degenerate wriggling modes for the two equal sphere model. The long arrows originating at the point of tangency for the two spheres is the orbital angular momentum while the shorter arrows represent the individual fragment spins.

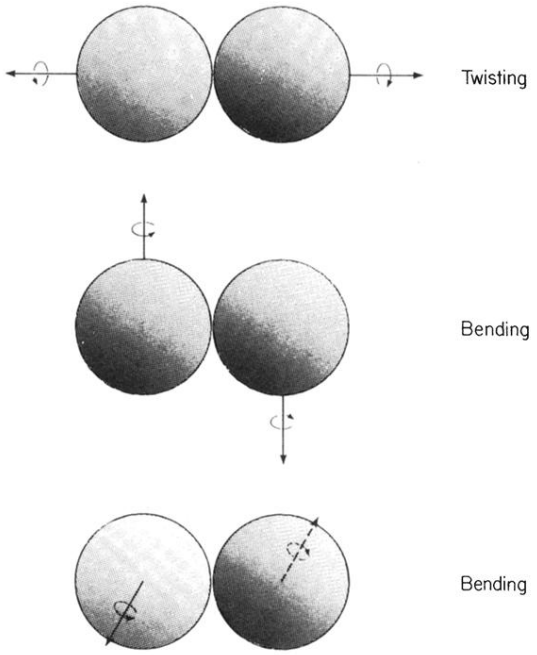

FIG. 6. Schematic illustrating the twisting and bending modes for the two-equal-sphere model. Note the pairwise cancellation of the fragment spins.